Pergamon

Int. J. Heat Mass Transfer. Vol. 38, No. 13, pp. 2403–2410, 1995

0017-9310/95 $9.50+0.00

0017-9310(94)00363-7

Local heat transfer, solids concentration and erosion around membrane tubes in a cold model circulating fluidized bed

C. LOCKHART, J. ZHU,† C. M. H. BRERETON, C. J. LIM and J. R. GRACE‡

Department of Chemical Engineering, University of British Columbia, Vancouver, British Columbia, Canada V6T 1Z4

(*Received* 25 *January* 1994 *and in final form* 28 *November* 1994)

Abstract—Measurements of local solids concentration, heat transfer and erosion were obtained in a 152 mm diameter × 9.3 m tall circulating fluidized bed operated at room temperature with 200 μm sand particles at a superficial gas velocity of 7.0 m s^{-1} with different solids circulation rates. Local solids concentrations were found to be higher in the fin region than on the crests of membrane tubes. For the small heat transfer surfaces investigated, this led to higher local heat transfer coefficients in the fin region, a trend which is the reverse of that for long heat transfer surfaces. Erosion rates were higher on the tube crests than on the fins.

INTRODUCTION

In the last decade, circulating fluidized bed technology has been applied to such processes as solid fuel combustion, calcination and gasification. Removal of heat produced during combustion is essential for fluidized bed boilers, and a number of studies of heat transfer have been reported recently. These have been reviewed by Grace [1, 2], Glicksman [3] and Leckner [4].

Previous studies in a pilot circulating fluidized bed combustor (CFBC) carried out by this research group [5, 6] have shown that the time average heat transfer coefficient increases almost linearly with bed suspension density calculated from the pressure drop gradient measured at the given height. Using an instantaneous heat transfer probe, Wu *et al.* [7] found that the local instantaneous heat transfer coefficient on a smooth surface is directly related to the local solids concentration, with a higher heat transfer coefficient corresponding to a higher local solids concentration. Since it is well known that radial solids distribution is not uniform in circulating fluidized beds [8], it is not surprising that heat transfer coefficients vary with lateral location of a heat transfer surface [6].

While some studies have been reported regarding radial solids concentration distribution, the relationship between the cross-sectional averaged solids concentration and the local solids concentration at the wall is dependent on the geometric configuration of the reactor. For example, the local solids concentration distribution in the wall region of a circulating fluidized bed with membrane tubes (as used in CFBC units used for electrical power generation) appears to differ from that without membrane tubes [2, 7]. It is expected that the presence of membrane tubes on the wall will affect the local solids concentration in the wall region, hence affecting heat transfer. Therefore, it is important to study the local solids concentration variation and the local heat transfer variation at the same time.

In the present study, the local solids concentration distribution around the membrane wall and local heat transfer coefficients at different points on the membrane tube assembly were measured simultaneously to determine the local solids concentration distribution in the presence of membrane tubes and to determine the effect of solids concentration variation on heat transfer.

EXPERIMENTAL SET-UP AND MEASUREMENT TECHNIQUES

The cold model circulating fluidized bed apparatus is shown in Fig. 1. It consists of a riser of 9.3 m height and 152 mm inside diameter, two cyclones, a solids return column and an L-valve for solids feeding. The entire unit is constructed of 6.4 mm thick transparent polyacrylic material, except for the primary cyclone which is constructed from steel to resist erosion. The air distributor is a multi-orifice plate with an open area of 19%. A 914 mm tall section equipped with polyacrylic membrane tubes was mounted beginning 4.11 m above the air distributor (see Fig. 1). Seven 19 mm (3/4″) and five 32 mm (1 1/4″) diameter half tubes were mounted onto each half of the wall of the

† Current address: Department of Chemical and Biochemical Engineering, University of Western Ontario, London, Ontario, Canada N6A 5B9.

‡ Author to whom correspondence should be addressed.

NOMENCLATURE

d_p	average particle size [μm]	U	superficial gas velocity [m s^{-1}]
G_s	solids circulation rate [kg m^{-2} s^{-1}]		

measuring section, with inter-tube spacing equal to the corresponding tube radii as shown in Fig. 2. The membrane tubes extended the entire length of the special section, with a smooth tapered transition at the top and bottom to the fully cylindrical sections above and below.

The heat transfer sensors employed the same principle as those used by Wu *et al.* [7, 9]. They consisted of thin platinum films deposited on glass pieces with a 9.5 mm radius of curvature, which were then mounted onto 19 mm diameter aluminum probe mounts. A thin film of platinum solution was first sprayed onto a rectangular area in the centre part of a piece of glass support, and then the platinum film was bonded to the glass by curing in a 650°C oven. The platinum film was then connected to a programmable power supply and a known reference resistor. The circuit designed for the heat transfer sensor is shown in Fig. 3. The platinum film functions simultaneously as a heater element and a temperature sensor. Its temperature is maintained constant and the instantaneous power dissipation from the sensor is measured by means of an IBM XT personal computer coupled to a Dash-8 A/D–D/A interface board. A guard heater was inserted on the back within the hollow aluminum probe mount to minimize heat loss from the back of the sensor and to limit temperature variation of the glass support. A 10 μm thick plastic film covered the platinum film to protect it from wear due to the particles. For more details of these sensors, see Wu *et al.* [7, 9].

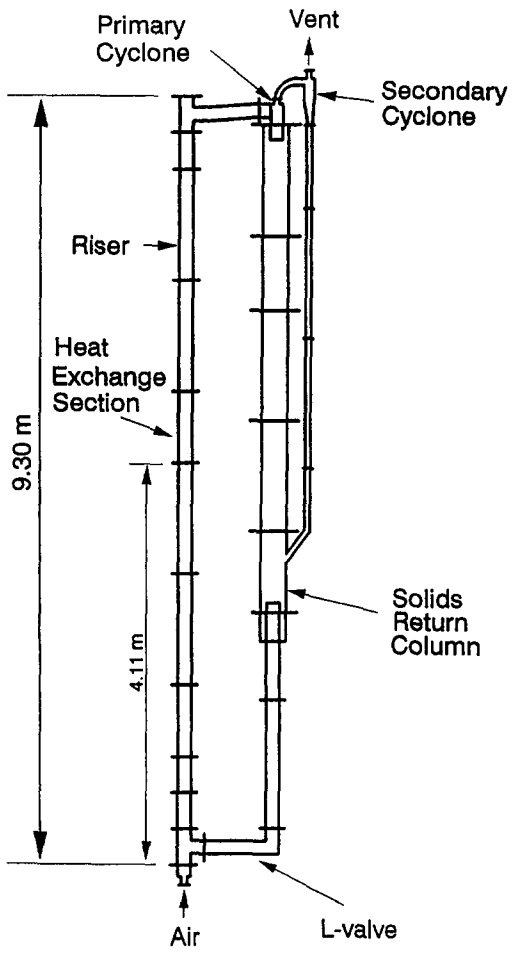

Fig. 1. Circulating fluidized bed experimental set-up.

Three such heat transfer sensors were used to measure local instantaneous heat transfer coefficients at three locations around the periphery of the membrane section. One sensor was located on the fin between two 32 mm half tubes (sensor No. 1), while the other two sensors were mounted on the crests of the 32 mm and 19 mm tubes (sensors Nos. 2 and 3), respectively (see Fig. 2). The new feature was that sensor Nos 2 and 3 were shaped in such a way that they matched the curvature of the two tubes of different diameters. All three sensors were mounted, with considerable care taken to ensure that the heat transfer surface was perfectly flush with the corresponding column or membrane inner surface since any misalignment could affect the local particle flow. The heat transfer area for sensor No. 1 was 6.9 mm high by 5.5 mm wide, while the areas for sensor Nos 2 and 3 were 7.9 mm high by 13.1 mm wide and 7.1 mm high by 10.6 mm wide, respectively. During the experiments, the temperatures of the sensor surfaces were maintained at 78°C and the temperature of the probe mounts were kept at a slightly lower temperature of 75°C.

A capacitance probe similar to that reported by Brereton and Grace [10] was used to measure local solids concentrations. As shown in Fig. 4, a stainless steel wire of 0.6 mm diameter was used as the live core, projecting 3 mm from a concentric 3.2 mm o.d., 2.2 mm i.d. stainless steel tube which acts as the other pole of the capacitor. The wire is insulated from the sheath by magnesium oxide thermocouple insulator. A 6.4 mm o.d. bushing was used to hold these components rigid. During the experiments, the capacitance probe was mounted horizontally and was traversed horizontally from the opposite side of the column to facilitate measurement of radial solids concentration profiles in the vicinity of the membrane surfaces.

Erosion probes are of the same shapes as the heat transfer sensors, with several layers of paint coated

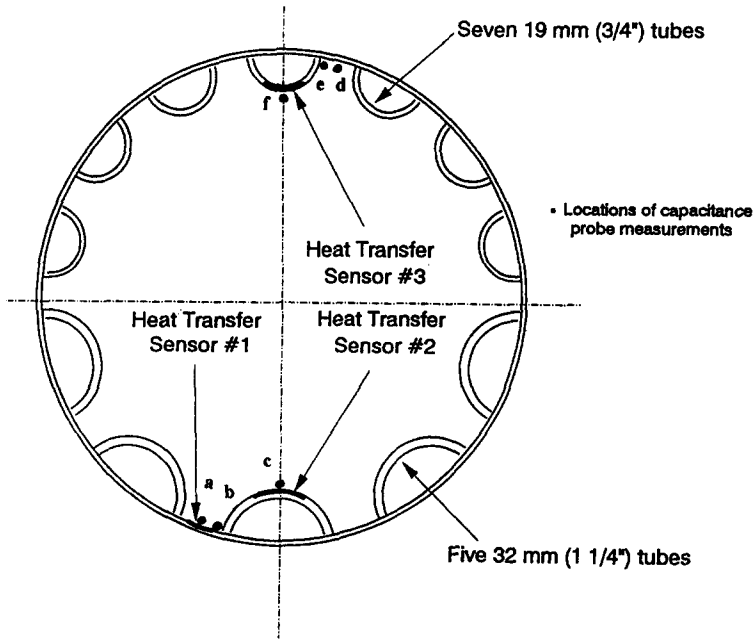

Fig. 2. Arrangement of model heat transfer tubes and locations of heat transfer sensors in the membrane section.

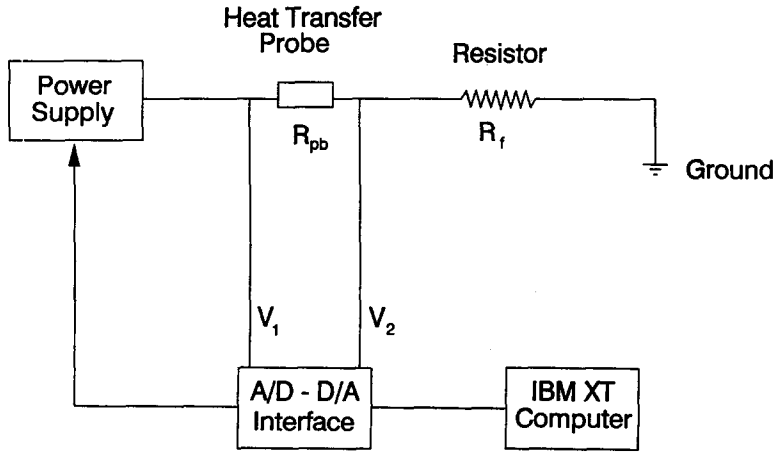

Fig. 3. Electrical circuit designed for the heat transfer sensor.

directly onto the surface of the aluminum holders. The probes were at the same positions as sensors 1, 2 and 3 in Fig. 2, with an additional position corresponding to the fin between two 19 mm tubes at the same height. The probe surfaces were again carefully aligned flush with the fin and membrane tube surfaces. A thin water-based air-brush paint was chosen after unsuccessful attempts with enamel-based and latex–acrylic based spray paint, since a very thin and uniform layer can be coated onto the probe by the air brush. Specially designed for artistic paintings, the air brush contained a small liquid reservoir and a tiny tube for air flow with an injection nozzle at the front end and a side branch extending into the reservoir. When compressed air was passed through the tube, paint was drawn by suction into the air flow and sprayed uniformly onto the object in front of the nozzle. The flow of paint could be adjusted by changing the needle position inside the nozzle and the air pressure. To ensure a uniform thickness for successive layers, the distance between the air brush and the probe surface and the duration of spraying were fixed for all layers painted. Five layers of the paint of different colours were sprayed in succession, and the relative erosion rate was expressed semi-quantitatively in term of how many layers had been removed. During the erosion tests, probes were removed at 3-h intervals for inspection and photography. At the end of the tests, photographs were divided into hundreds of squares and the colour of each square was recorded,

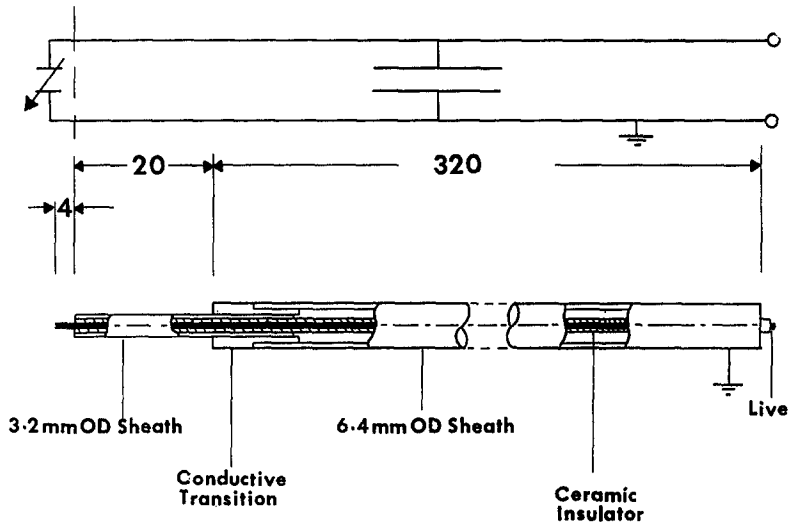

Fig. 4. Capacitance probe used for solids concentration measurements. (All dimensions in mm.)

by assigning numbers 1–5 to the successive layers. A measure of average relative erosion was then obtained by averaging the numbers recorded.

Ottawa sand having a density of 2650 kg m^{-3} and a mean diameter, d_p, of 200 μm was used as bed material. The superficial gas velocity, U, was maintained at 7.0 m s^{-1} for all runs. The solids circulation rates, G_s, and corresponding average suspension densities in the heat transfer section are given in Table 1.

SOLIDS CONCENTRATION RESULTS AND DISCUSSION

The capacitance probe was used to measure the local solids concentration at six locations just inside the periphery of the membrane wall section as shown by the lettered dots in Fig. 2. Measurements were obtained at three locations for both the 19 and 32 mm tubes, corresponding to the crest of the tube, the midpoint of the fin and the junction (or corner) between the tube and fin. All measurements were vertically mid-way up the membrane section, i.e. 4.57 m above the distributor plate. When measuring local solids concentrations, the tip of the capacitance probe was always 1 mm away from the nearest wall.

The measured time-mean local solids volumetric concentrations are given in Fig. 5, plotted against the cross-sectional average suspension density, estimated from the static pressure gradient. It is clearly shown that for both tubes the solids volumetric concentration at the junction between the fin and the tube is much higher than at the crest or at the centre of the fin. For higher solids suspension density, the local solids concentration can be as high as 40% in this region, approaching the packed bed concentration. One explanation for the higher solids holdup in the corners is that the existence of membrane tube has created a shielding effect to protect particles from being carried away easily. An alternative explanation is that the increased contact area between the particles and the wall in that region results in increased friction, thereby retarding particle downwards movement and increasing solids holdup. It is also noted from Fig. 5 that the solids holdup near the tube–fin junction for the 19 mm tube tends to be higher than for the 32 mm tube. The effect of shielding and/or particle-wall friction

Table 1. Cross-sectional average suspension density between 4 and 5 m above the distributor determined from pressure gradient with and without membrane tubes (superficial gas velocity: 7.0 m s^{-1}, particles: Ottawa sand of density 2650 kg m^{-3})

Solids circulation rate [kg m^{-2} s^{-1}]	Suspension density [kg m^{-3}] —without membrane wall* Mean particle size 171 μm	Suspension density [kg m^{-3}] —with membrane wall† Mean particle size 200 μm
39.5	17	25
43.0	20	47
50.5	29	69
59.0	48	91

* From Fig. 3.8 of Wu [11].
† This study.

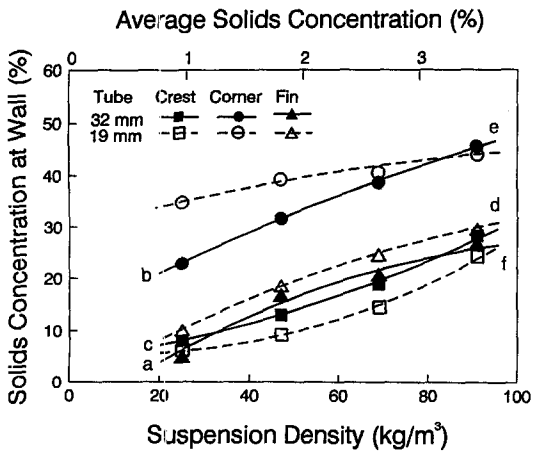

Fig. 5. Measured time-mean local solids concentration at different locations along membrane wall as a function of solids suspension density for $U = 7.0$ m s^{-1}. Letters on the lines refer to corresponding letters shown in Fig. 2.

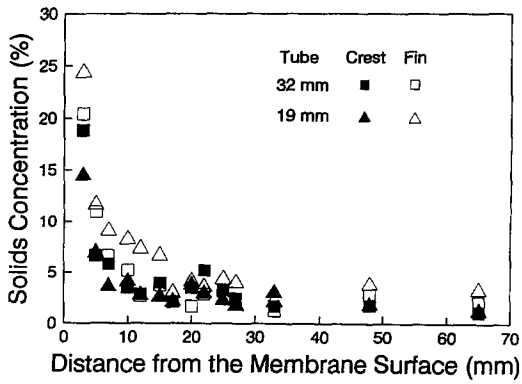

Fig. 6. Radial solids concentration profiles in the membrane section for $U = 7.0$ m s^{-1} and $G_s = 50.5$ kg m^{-2} s^{-1}.

appears to be stronger for the 19 mm tube due to its narrower fin width.

The solids concentrations at the mid-points of the two fins are also higher than at the crests of the two tubes. The fin region has more potential than the crest region to protect particles from being carried into the main stream by upflowing gas. The fin region for the 19 mm tube is more protected by the two neighbouring tubes.

As expected, increasing solids suspension density in the membrane section (by increasing solids flux through the riser) results in a higher solids holdup in the wall region including the fin, the corner and the crest. When we compare these results with earlier results [11] for average solids suspension density in a circular column without membrane tubes, the average solids suspension density in the membrane tube section is considerably higher with membrane tubes present under similar operating conditions (see Table 1). While some of the differences may be attributed to different mean particle sizes, the extent of the density differences suggests that the presence of membrane tubes not only increases the local solids holdup in the wall region, but also increases the total solids holdup in that section of the riser for a given solids circulation rate. This conclusion is supported by experimental observations which indicate that the solids holdup is significantly less in the section immediately above the membrane section than in the membrane section itself.

Radial time-mean solids concentration profiles have also been measured by traversing the capacitance probe from the wall to the centre of the column along a radius, taking measurements at 3-mm increments. The results for the crests and fins of the two probes and a solids circulation rate of 50.5 kg m^{-2} s^{-1} are plotted in Fig. 6. Local solids concentration is much higher near the wall than in the core region, in agreement with the core–annulus structure reported by other researchers for fully cylindrical columns [8, 12].

HEAT TRANSFER RESULTS AND DISCUSSION

As described above and shown in Fig. 2, heat transfer sensors were used to measure local instantaneous heat transfer coefficients at three positions. The capacitance probe was placed 3 mm away from the centre of the heat transfer sensors to measure the local solids concentration. Time-mean results from the three heat transfer sensors are presented in Fig. 7, plotted against cross-sectional average suspension density. Figure 7 clearly shows that heat transfer is significantly higher at the fin than at the crest of the 32 mm tube, presumably due to increased solids concentration along the fin region as presented in Fig. 5. The heat transfer coefficients are very similar in Fig. 7 for the crests of the two sizes of tube.

As reported by Wu *et al.* [9], local heat transfer coefficient is a strong function of solids suspension density (i.e. cross-sectional average solids holdup) inside the riser, with increasing solids suspension den-

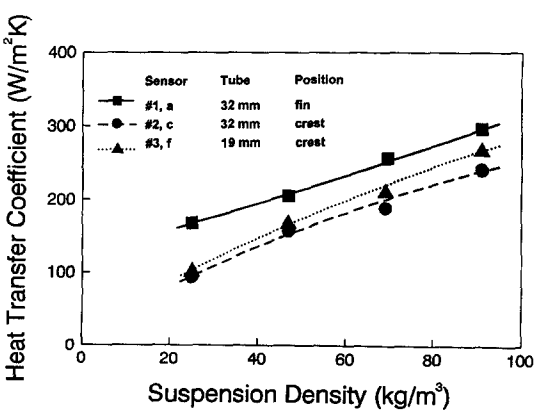

Fig. 7. Measured local time-mean heat transfer coefficients at the membrane wall as a function of suspension density for $U = 7.0$ m s^{-1}. Numbers and letters refer to local heat transfer sensors and capacitance probe positions, respectively indicated in Fig. 2.

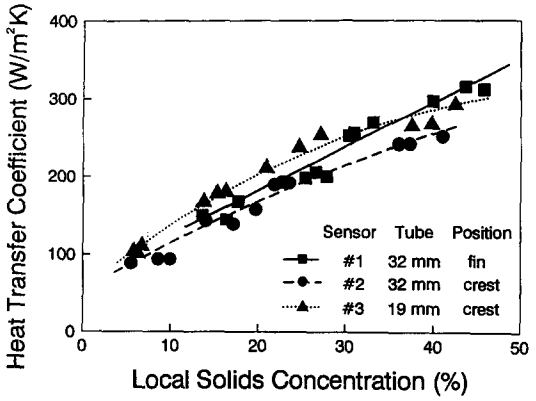

Fig. 8. Measured local time–mean heat transfer coefficients plotted against corresponding local time–mean solids concentration for $U = 7.0$ m s^{-1} and $G_s = 39.5$, 43.0, 50.5 and 59.0 kg m^{-2} s^{-1}.

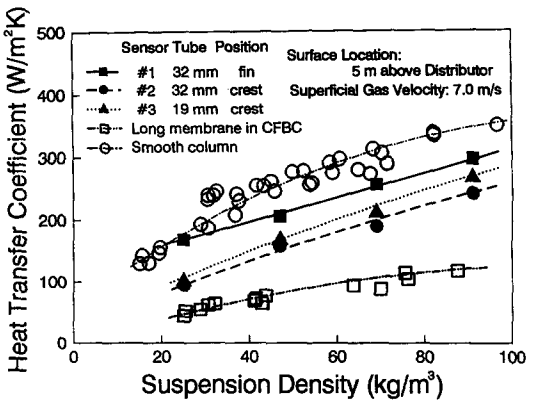

Fig. 10. Heat transfer coefficients vs cross-sectional average suspension density for the membrane section in this study ($U = 7.0$ m s^{-1} and $d_p = 200$ μm), shown by blacked-in symbols, compared with those measured by Wu [11], shown by open symbols, in a fully circular column ($U = 7.0$ m s^{-1} and $d_p = 177$ μm) and in a pilot circulating fluidized bed combustor ($U = 4.5$–7.5 m s^{-1} and $d_p = 188$ μm).

sity giving higher heat transfer coefficient. The same trend is observed in Fig. 7, where the heat transfer coefficients for all three locations are shown to increase with increasing solids suspension density. Figure 8 shows that the local time–mean heat transfer coefficient also has a nearly linear relationship with the local time–mean solids concentration determined by the capacitance probe. One would, of course, expect that it is the local solids concentration that actually affects the local heat transfer coefficient. While the cross-section average solids suspension density calculated from pressure drop measurement is useful for correlating heat transfer, this is probably because the local solids concentration rises and falls with the overall cross-section average value for a given column geometry.

To demonstrate the effect of wall roughness on heat transfer, a section of horizontal 2 mm wire was glued onto the smooth membrane wall along the periphery, either 5 mm above the three heat transfer sensors (see insert on Fig. 9) or 5 mm below the sensors. With the volume occupied by the glue, this created a 3-mm thick object protruding into the flow, causing a disturbance. As shown in Fig. 9, the results indicate that the disturbance created by the thin wire did not change the local heat transfer coefficient significantly. However, the influence may become more noticeable if the object protrudes further. A 50% increase in heat transfer has been reported by Andersson and Leckner [13] when an obstacle was inserted 0.1 m into a combustor 0.5 m above a heat transfer sensor. The influence may also become significant when the protruding object is much closer to the heat transfer sensor. A decrease of 30% in heat transfer rate has been noted [2] when a 1 mm wire was placed immediately above the heat transfer sensor. As pointed out by Lints and Glicksman [14], an obstruction of one particle diameter in thickness attached to the wall can disrupt the flow of particles in the wall region. The effect of obstructions on heat transfer depends, however, on the relative distance from the obstruction to the heat transfer measurement point. When the obstruction is very close to and above the heat transfer probe, it may deflect the particle flow away from the probe so that a decrease in heat transfer rate occurs [2]. On the other hand, when the obstruction is some distance above the heat transfer probe, the obstruction may enhance particle renewal in the region immediately above the heat transfer probe so that the heat transfer rate increases [13]. It is well known that particle renewal in the wall region plays a very important role in bed-to-wall heat transfer [11, 14]. In comparing these experimental findings, it is important to realize that there is no thermal boundary layer to disturb in cold model tests; hence disturbing the flow will not initiate thermal renewal.

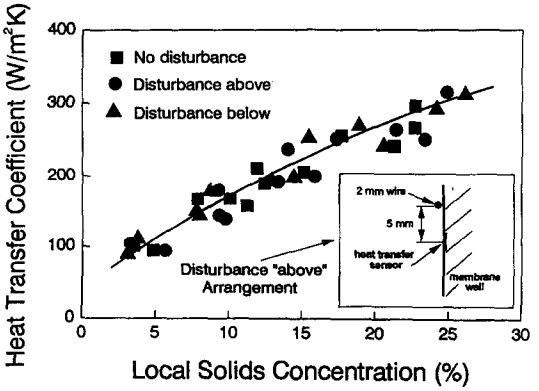

Fig. 9. Effect of disturbance on local time–mean heat transfer coefficients measured in the membrane section for $U = 7.0$ m s^{-1} and $G_s = 39.5$, 43.0, 50.5 and 59.0 kg m^{-2} s^{-1}.

The current results are compared with results from Wu [11] for both a cold model circulating fluidized bed and a pilot scale circulating fluidized bed combustor in Fig. 10. Compared with results obtained in the pilot circulating fluidized bed combustor with membrane

tubes operating under similar conditions ($U = 4.5$ to 7.0 ml s^{-1}, $d_p = 188$ μm), the present study gives significantly higher heat transfer coefficients. This is quite understandable since a local heat transfer coefficient is measured here, while values averaged over a length of 1.2 m were obtained in the Wu study. As shown by Wu *et al.* [5] and Glicksman [3], the average heat transfer coefficient for a heat transfer surface depends strongly on the vertical length of the surface, since heat transfer depends not only on local solids concentration but also on the time which the solids have been in contact with the heat transfer surface. Since solids predominantly move downwards along the column wall, only the top section of the tube is in contact with fresh solids while further down the solids approach thermal equilibrium with the tube.

Local heat transfer coefficients obtained by Wu [11] at room temperature in the same column with similar operating conditions ($U = 7.0$ m s^{-1}, $d_p = 177$ μm, 4.0 and 8.6 m above the distributor) with no membrane surface are also plotted in Fig. 10, against the suspension density in the sections where heat transfer was measured. It is seen that, except for low suspension densities, the heat transfer coefficients for the smooth circular cylindrical column are somewhat greater than those at the crests and the fins for the membrane surface. Part of this difference may be due to the fact that the particles were somewhat finer in the earlier studies. Another factor may be that the cylindrical column has a smaller perimeter than the column equipped with membrane tubes so that the heat transfer coefficient, defined with respect to surface area, is lower for the latter even though the heat transfer rate is increased. There could also be differences in the configuration and spacing of streamers adjacent to cylindrical and membrane surfaces.

One other factor to consider is that the particle circulation rate is significantly higher in the smooth column than in the column with membrane tubes in order to have the same suspension density in the measurement section (4–5 m above the distributor) due to the effect of membrane tubes on the gas–solid flow. As shown in Table 1, a solids circulation rate of 43 kg m^{-2} s^{-1} results in a suspension density of 47 kg m^{-3} in the membrane section 4–5 m above the distributor in the column equipped with membrane tubes. To achieve a similar suspension density at the same height in the smooth column, i.e. 48 kg m^{-3}, the solids circulation rate has to be increased to 59 kg m^{-2} s^{-1}. This indicates that for the same solids suspension density, there are many more particles travelling through the measured section in the smooth column than in the same section with membrane tubes. This increased particle throughput may well lead to higher local concentrations near the wall and/or more lateral transfer of particles, thereby contributing to the higher heat transfer coefficient in the smooth section. To examine the role of solids circulation rate, it is of interest to compare the results on the basis of solids circulation rates.

Heat transfer coefficients obtained with and without the membrane section are plotted against the solids circulation rate in Fig. 11. The superficial gas velocity was kept at 7.0 m/s and the heat transfer probe was between 4 and 5 m above the distributor for all the data plotted. (Heat transfer coefficients obtained by Wu [11] at 8.6 m above the distributor are not included in Fig. 11.) When compared in this manner, i.e. for the same solids circulation rate and superficial gas velocity, the heat transfer coefficient without membrane is comparable with the heat transfer at the crests of the membrane tubes. The heat transfer at the fin is, however, higher. This comparison indicates that the solids circulation rate or some factor which relates suspension density to column geometry plays an important role in particle-to-wall heat transfer; cross-sectional average suspension density alone cannot correlate the heat transfer coefficient.

It must be recognized that the fin has a higher heat transfer coefficient than the crest for short heat transfer surfaces, but this may well not be true for long heat transfer surfaces. This is because particles are relatively protected and sweep much further along the fins than along the crests [11]. Hence, particles in contact with the fins are more likely to approach thermal equilibrium with the surface than particles near the crests. Therefore, long membrane surfaces have higher heat transfer coefficients for the crests than for the fins, and this has been found experimentally by Leckner and Andersson [15] and by Golriz [16].

EROSION RESULTS AND DISCUSSION

The results of the erosion study are shown in Fig. 12, where the number of eroded layers is plotted against the period of operation. Erosion was more severe at the crest of the tubes than along the fin and was higher on the crest of the 32 mm tube than on the 19 mm tube. The higher erosion on the crests no doubt arises because they are more exposed to impacts by

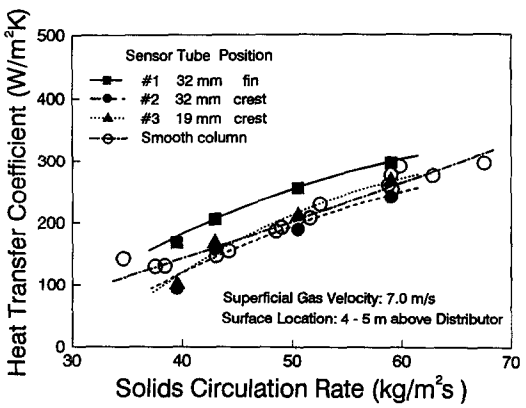

Fig. 11. Heat transfer coefficients vs solids circulation rate for the membrane section in this study ($U = 7.0$ m s^{-1} and $d_p = 200$ μm), shown by blacked-in symbols, compared with those measured by Wu [11], shown by open symbols, in a fully circular column ($U = 7.0$ m s^{-1} and $d_p = 177$ μm).

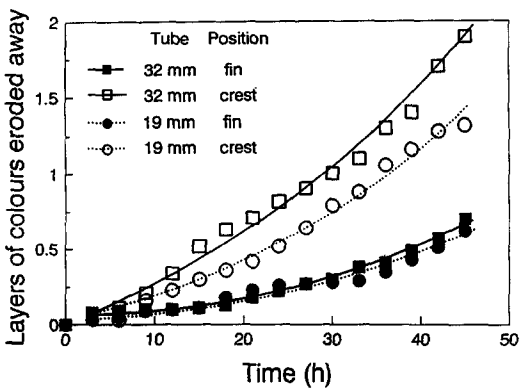

Fig. 12. Relative erosion rate of heat transfer surface at different positions in the membrane section.

particles having substantial horizontal components of velocity, whereas the fins are protected by layers of particles travelling parallel to the surface. As expected, the erosion rate here was considerably less than that obtained in an earlier erosion study by one of the authors with horizontal tubes and larger particles in a bubbling fluidized bed [17].

CONCLUSIONS

Local solids concentrations and local heat transfer coefficients in a laboratory scale circulating fluidized bed operated at room temperature are higher in the protected fin region of membrane heat transfer surfaces than on the crests of the tubes. The membrane section results in higher cross-sectional average suspension densities than in a corresponding fully circular (smooth) walled vessel at the same solids circulation rate. Possibily as a result, local heat transfer coefficients tend to be higher for circular walls when compared at equal overall suspension densities, but somewhat lower when compared at equal solids circulation rates. Local time–average heat transfer coefficients correlate well with local time–average local solids concentrations. Erosion rates were higher on the crests of tubes than on the fins.

Care must be exercised in applying these results to long heat transfer surfaces, where higher heat transfer coefficients are found on the crests than on the fins due to greater renewal of particles on the crests. It may also be misleading to extrapolate these results to larger units, where downward-moving wall layers of particles may be considerably deeper than the tube radius. Variations of local heat transfer coefficients with location need to be considered in modelling heat transfer in circulating fluidized bed boilers.

Acknowledgements—The authors are grateful to Energy, Mines and Resources Canada and to the Natural Sciences and Engineering Research Council of Canada for financial assistance.

REFERENCES

1. J. R. Grace, Heat transfer in circulating fluidized beds. In *Circulating Fluidized Bed Technology* (edited by P. Basu), pp. 63–80. Pergamon Press, New York (1986).
2. J. R. Grace, Heat transfer in high velocity fluidized beds, *Proceedings of the Ninth International Heat Transfer Conference*, Vol. 1, pp. 329–339 (1990).
3. L. R. Glicksman, Circulating fluidized bed heat transfer. In *Circulating Fluidized Bed Technology* II (edited by P. Basu and J. F. Large), pp. 13–29. Pergamon Press, New York (1988).
4. B. Leckner, Heat transfer in circulating fluidized bed boilers. In *Circulating Fluidized Bed Technology* III (edited by P. Basu, M. Horio and M. Hasatani), pp. 27–37. Pergamon Press, New York (1991).
5. R. L. Wu, C. J. Lim, J. Chaouki and J. R. Grace, Heat transfer from a circulating fluidized bed to membrane waterwall surfaces, *A.I.Ch.E.J.* **33,** 1888–1893 (1987).
6. R. L. Wu, J. R. Grace, C. J. Lim and C. M. H. Brereton, Suspension-to-surface heat transfer in a circulating fluidized bed combustor, *A.I.Ch.E.J.* **35,** 1685–1691 (1989).
7. R. L. Wu, C. J. Lim, J. R. Grace and C. M. H. Brereton, Instantaneous local heat transfer and hydrodynamics in a circulating fluidized bed, *Int. J. Heat Mass Transfer* **34,** 2019–2027 (1991).
8. W. Zhang, Y. Tung and F. Johnsson, Radial voidage profiles in fluidized beds of different diameters, *Chem. Engng Sci.* **46,** 3045–3052 (1991).
9. R. L. Wu, C. J. Lim and J. R. Grace, The measurement of instantaneous local heat transfer coefficients in a circulating fluidized bed, *Can. J. Chem. Engng* **67,** 301–307 (1989).
10. C. M. H. Brereton and J. R. Grace, Microstructural aspects of the behaviour of circulating fluidized beds, *Chem. Engng Sci.* **48,** 2565–2572 (1993).
11. R. L. Wu, Heat transfer in circulating fluidized beds, Ph.D. Dissertation, The University of British Columbia, Vancouver, Canada (1989).
12. B. Herb, S. Dou, K. Tulza and J. C. Chen, Solid mass fluxes in circulating fluidized beds, *Powder Technol.* **70,** 197–205 (1992).
13. B. Å. Andersson and B. Leckner, Experimental methods of estimating heat transfer in circulating fluidized bed boilers, *Int. J. Heat Mass Transfer* **35,** 3353–3362 (1992).
14. M. C. Lints and L. R. Glicksman, Parameters governing particle-to-wall heat transfer in a circulating fluidized bed. In *Circulating Fluidized Bed Technology IV* (edited by A. A. Avidan), pp. 297–304. AIChE, New York (1994).
15. B. Å. Andersson and B. Leckner, Local lateral distribution of heat transfer on tube surface of membrane walls in CFB boilers. In *Circulating Fluidized Bed Technology IV* (edited by A. A. Avidan), pp. 311–318. AIChE, New York (1994).
16. M. R. Golriz, Influence of wall geometry on local temperature distribution and heat transfer in circulating fluidized bed boilers. In *Circulating Fluidized Bed Technology IV* (edited by A. A. Avidan), pp. 693–700. AIChE, New York (1994).
17. J. Zhu, Ph.D. Research Proposal, The University of British Columbia, Vancouver, Canada (1985).